Δ9-THC increases endogenous AHA1 expression in rat cerebellum and may modulate CB1 receptor function during chronic use

Catalin M. Filipeanu[*], **Jesse J. Guidry**, **Stuart T. Leonard**, and **Peter J. Winsauer**

Department of Pharmacology and Experimental Therapeutics, Louisiana State University Health Sciences Center, New Orleans, Louisiana, USA

Abstract

To characterize the long-term effects of adolescent marijuana abuse, we performed a proteomic analysis of cerebellar extracts from adult female rats with and without ovariectomy that were treated with Δ9-THC for 40 days during adolescence. Six proteins were found to significantly differ among the four treatment groups, with Δ9-THC and ovarietcomy decreasing the mitochondrial proteins, pyruvate carboxylase and NADH dehydrogenase, whereas the levels of putative cytosolic molecular chaperones NM23B, translationally controlled tumor protein, DJ-1 and AHA1 were increased. We further analyzed the effects of AHA1, a HSP90 co-chaperone, on CB1R and CB2R trafficking and signaling in transfected HEK293T and Neuro-2A cells. In HEK293T cells, AHA1 overexpression enhanced plasma membrane levels of CB1R and increased CB1R-mediated effects on cAMP levels and on MAPK phosphorylation. AHA1 overexpression also enhanced cell surface levels of endogenous CB1R and the effects of Δ9-THC on the cAMP levels in Neuro-2A cells. In contrast, overexpression of AHA1 did not affect the subcellular localization and signaling of CB2R. Our data indicate that chronic Δ9-THC administration in adolescence altered the endogenous levels of specialized proteins in the cerebellum, such as AHA1, and that this protein can change CB1R cell surface levels and signaling.

Keywords

Δ9-THC; cerebellum; proteomic analysis; AHA1; CB1R; molecular chaperones

Introduction

According to the National Survey on Drug Use and Health, over 40.1% of all Americans have tried marijuana at least once in their lifetime, meaning that this is the most frequently used illegal drug in the United States (Substance Abuse and Mental Health Services Administration, National Survey on Drug Use and Health: National Findings, September 2006). The main psychoactive component of marijuana is Δ9-THC, which produces a variety of pharmacological and physiological effects (Mechoulam, 1986). In addition,

[*]Corresponding author, cfilip@lsuhsc.edu, tel: 1 504 568 4514, fax: 1 504 568 2361, Department of Pharmacology and Experimental Therapeutics, Louisiana State University Health Sciences Center, 1901 Perdido Street, New Orleans, Louisiana, LA-70112, USA.

Disclosure/conflict of interest: The authors have no conflict of interest.

mammals have an endogenous cannabinoid system consisting of endogenous ligands (i.e., anandamide and 2-arachidonylglycerol) and the enzymes involved in the synthesis and degradation of these endocannabinoids (Cabral et al., 2008; Makie, 2008; Turu and Hunyady 2010; Rozenfeld, 2011). However, fine differences have been reported between the effects of 9-THC and endogenous cannabinoids at the molecular and the organism level, possibly because they activate different cellular signaling pathways (Childers 2006; Heinman et al., 2008). The biological effects of all cannabinioids are mediated by interactions with specific plasma membrane receptors that are members of the G-protein coupled receptor superfamily (GPCR), with CB1 (CB1R) and CB2 (CB2R) receptors being the best characterized subtypes (Cabral et al., 2008; Makie, 2008; Bosier et al., 2010; Turu and Hunyady, 2010). In addition, the former orphan receptors, GPR55 and GPR119, were proposed to be activated by cannabinoid-like drugs, but whether they are 'true' cannabinoid receptors is still a matter of debate (Godlewski et al., 2009).

The amplitude of the cellular response to cannabinoids is directly correlated with the number of cannabinoid receptors expressed by the cells. GPCR expression is a highly regulated process, involving the synthesis of new receptors, the intracellular trafficking of these receptors to the functional site, as well as receptor internalization (constitutive or induced by the ligands), followed by degradation in the lysosomes or proteasomes (Duvernay et al., 2005; Dong et al., 2007). Within the GPCR family, CB1R and CB2R present certain characteristics, not common to other members. Likewise, the CB1R can modulate cellular signaling when localized not only at the plasma membrane, but also when localized in the intracellular compartments (Leterrier et al., 2005; Rozenfeld and Devi, 2008; Rozenfeld 2011). In fact, most cannabinoid ligands are highly lipophilic and readily diffuse across the plasma membrane to activate intracellularly localized receptors (Oz, 2006; Reggio, 2010). The signaling events mediated by CB1R may differ according to the subcellular localization of the receptor (Rozenfeld and Devi 2008; Cudaback et al., 2010). Further, CB1R undergo constitutive recycling from early endosomes to plasma membrane, and long-term exposure to ligand may result in switching the cellular signaling pathways mobilized by CB1R activation (Filipeanu et al., 1997; Rozenfeld and Devi, 2008; Rozenfeld, 2011).

Each of the steps in GPCR expression and degradation is controlled by interactions with specialized proteins known under the generic name of molecular chaperones (Dong et al., 2007; Durham and Hall, 2009; Cooray et al., 2009). Molecular chaperones are localized in the endoplasmic reticulum, cytosol, Golgi apparatus or lysosomes and by directly interacting with the chaperoned protein determine its trafficking and functional availability. Many such molecular chaperones were described for the GPCR family, some of which are common for all members (i.e., calnexin for the maturation and exit from the endoplasmic reticulum, and β-arrestin for receptor internalization), whereas other molecules are specific for certain GPCR (Dong et al., 2007; Tuusa et al., 2007; DeWire et al., 2007). For instance, the endosomal localization of CB1R in resting cells was found to depend on interactions with adaptor protein AP-3 (Rozenfeld and Devi, 2008), whereas the activation of $G_{\alpha i}$-Rac1 pathway by CB2R requires the receptor interaction with HSP90 (He et al., 2007). Further, we recently demonstrated that HSP90 modulates the temperature-dependent intracellular trafficking of α_{2C}-adrenergic receptor (Filipeanu et al., 2011). In addition, downregulation of AHA1 levels enhanced the cell surface levels of CFTR 508 mutant (Wang et al., 2006),

and inhibition of HSP90 activity decreased the maturation rate of insulin and nicotinic receptors (Ramos et al., 2007; Luo et al., 2008). These data indicate that the intervention of molecular chaperones, particularly HSP90 and its co-chaperones, may actively control the cellular levels of specific GPCR. Despite these data at the cellular level, still very little is known regarding the effects of chronic marijuana on the expression and signaling of CB1R and CB2R *in vivo*, or about the changes induced by 9-THC on the levels and the activity of molecular chaperones involved in the trafficking and degradation of these receptors. In an attempt to address this question, we recently analyzed the long-term effects of chronic 9-THC during adolescence in female rats by treating control and ovariectomized females for 40 days in adolescence, followed by analysis of the behavioral response as adults (Winsauer et al., 2011). The presence or absence of ovarian hormones in females was of interest as a cofactor because ovarian hormones have direct and indirect influences on maturation (Matsumoto et al., 1990) and published data indicate that the ovarian hormone estrogen can alter the effects of 9-THC on learning in female rats and alter the binding of cannabinoid ligands in brain areas that are critical for learning such as the hippocampus (Daniel et al., 2002; Winsauer et al., 2011). For these reasons, and because there is a paucity of data regarding the effects of 9-THC using female models (Pope et al., 1997), all of our behavioral experiments used female rats and involve the presence or absence of ovarian hormones in 9-THC-treated subjects. The cerebellum is one of the areas of the brain with the densest expression of cannabinoid receptors (Herkenham et al., 1990; 1991) and may be involved in the rate-decreasing (i.e., motor) effects observed by us (Winsauer et al., 2011).

In the present work, we extended this investigation by conducting a proteomic analysis of cerebellar extracts from the four animal groups used in the previous study. The endogenous expression of six proteins was found to be changed under these conditions. Out of these six proteins, we selected a specific co-chaperone of HSP90, AHA1 (activator of heat shock 90kDa protein ATPase homolog 1, Lotz et al., 2003; Wang et al., 2006), to examine its role in the modulation of CB1R and CB2R trafficking and signaling at the cellular level. We found that increases in the cellular levels of AHA1 specifically enhanced CB1R activity, but did not change the cell surface levels and the activity of CB2R. The present data strongly indicate that chronic marijuana use leads to modifications in the expression and activity of putative molecular chaperones, which then impact the long-term effects of cannabinoid receptor expression and signaling.

Experimental Procedures

Antibodies and chemicals

The sources of the antibodies used in the present study were as follows: anti-CB1R and anti-CB2R antibodies were from Cayman, anti-hemagglutinin (anti-HA) was from Santa Cruz, anti-AHA1 antibody was from Abnova, anti-HSP90α and anti-HSP90β antibodies were from Enzo Lifesciences, secondary anti-mouse and anti-rabbit antibodies were from Perkin Elmer, Alexa Fluor 594-labeled anti-mouse and anti-rabbit and anti-mouse antibodies and 4,6-diamidino-2-phenylindole were obtained from Invitrogen. The 9-THC was provided by the National Institute on Drug Abuse. OPD[o-Phenylenediamine] and isobutylmethylxanthine (IBMX) were from Sigma-Aldrich and forskolin was from Tocris.

Subjects

Sixteen of the thirty-one female Long-Evans rats (Harlan Sprague Dawley, Indianapolis, IN) used previously to determine the effects of hormone status and adolescent administration of ^{9}-THC on behavior and on CB-1 receptor levels (Winsauer et al., 2011) served as subjects for the present study. Subjects arrived on postnatal day (PD) 21 and were housed with a standard diet of rodent chow and *ad libitum* water until PD 30 when all the subjects were either ovariectomized or underwent a sham surgery. Female rats generally recover fully within 2 days after surgery. Food restriction was instituted at this time to maintain the compatibility of the treated groups (i.e., subjects were maintained at approximately 90% of their free-feeding weights while allowing for a gain of 5 grams per week to control for normal growth). The colony room was maintained throughout testing at $21 \pm 2°$ C with 50 ± 10% relative humidity on a 14L:10D light/dark cycle. All subjects were maintained in accordance with the Institutional Animal Care and Use Committee, Louisiana State University Health Sciences Center, and in compliance with the recommendations of the National Research Council in the Guide for the Care and Use of Laboratory Animals (National Research Council, 1996).

Administration of Saline or ^{9}-THC

From PD 35 to PD 75, both ovariectomized and intact (sham surgery) subjects received a single injection of either 5.6 mg/kg of ^{9}-THC or saline intraperitoneally (i.p.) at the same time each day, yielding 4 treatment groups with respect to hormone status and chronic ^{9}-THC administration (i.e., intact/saline, intact/THC, OVX/saline and OVX/THC). On PD 76 (beginning of adulthood), all of the treatment groups began training to respond under a multiple schedule of repeated acquisition and performance of response sequences (Thompson and Moerschbaecher, 1978).

Protein preparation for two-dimensional gel electrophoresis (DIGE)

Around PD 261, the subjects were sacrificed and the brain was dissected as described previously (Winsauer et al., 2011). For analysis, cerebellar sections were harvested into 7M Urea, 2M Thiourea, 4%CHAPS, 20% glycerol. These mixtures were sonicated at 25% amplitude for 30 seconds on ice. The resulting mixture was subjected to a brief centrifugal step before determining protein concentration using Bradford method. DIGE labeling and analysis was performed as previously described using a common standard (Alban et al., 2003). Fluorophore-labeled protein gels were scanned using a Typhoon 9400 Variable Mode Imager at 100 μm resolution. CyDyes are optimally detected using the following wavelength settings: Cy2, excitation 488 nm, emission 520 nm; Cy3, excitation 532 nm, emission 580 nm; Cy5, excitation 633 nm, emission 670 nm. Spot detection and quantification were performed using DeCyder differential analysis software DIA, Version 5.0 (GE Healthcare). Gels were then post-stained with Sypro Ruby, and images were captured again using a Typhoon 9400 Variable Mode Imager.

Protein Identification by Liquid Chromatography – Mass Spectrometry (LC-MS) and MS Analysis

Protein spots of interest were excised using the Ettan Spot Handling Work station with a 2-mm diameter spot-picking head. Gel spots were cut, de-stained and then digested with trypsin. The resulting peptide mixture was loaded on a Dionex PepMap C18 trap column and was separated by a New Objective reversed phase C18 Picofrit column/emitter. Peptide mass was determined by a Thermo-Fisher LTQXL linear ion trap mass spectrometer (Waltham, MA, USA) coupled with an Eksigent nanoLC. The raw data were analyzed by the Mascot search engine V2.2 against the rat SwissProt database (false discovery rate <5%) to generate a list of possible proteins for that gel spot.

Cell culture and transient transfection

HEK293T cells and Neuro-2A cells were cultured in DMEM with 10% fetal bovine serum, 10 units/ml penicillin, and 100 μg/ml streptomycin. Transient transfection of the HEK293T and Neuro-2A cells was performed using LipofectAMINE 2000 reagent (Invitrogen), in DMEM with no antibiotics and FBS at ~80% conflueny. After six hours the cells were trypsinized and plated at a density of 1×10^6 cells/well in 6-well plates for western blot experiments, 5×10^5 cells/well in 12 well-plates for ELISA experiments and 25×10^4 cells/well in 24-well plates for cAMP determinations.

Co-immunoprecipitation

The experiments were carried exactly as described previously (Filipeanu et al., 2011). Two days after transfection, the cells were lysed in a buffer containing 50 mM Tris–HCl, pH 7.4, 150 mM NaCl, 1% NP-40, 0.5% sodium deoxycholate, 0.1% SDS and Complete Mini protease inhibitor cocktail. The supernatant was cleared by centrifugation and incubation with 50 μl of protein A/G Sepharose, followed by incubation with anti-CB1R (5μg) antibodies overnight at 4°C. The protein complexes were recovered with 50 μl protein A/G Sepharose and further processed by western blot.

Western Blotting

Western blot analysis of protein expression was performed as described (Filipeanu et al., 2004; Filipeanu et al., 2011). The samples were separated by 10% SDS-PAGE, followed by transfer onto PDVF membranes. After exposure to specific primary and secondary antibodies, the protein levels were visualized using Fuji Film luminescent image analyzer (LAS-1000 Plus) and quantified using the Image Gauge program (V 3.4).

cAMP determinations

cAMP concentrations were measured using a cAMP enzymeimmunoassay system (Cayman) as described (Filipeanu et al., 2006; Filipeanu et al., 2011). HEK293T cells on 10 cm^2 dishes were transfected with 3 μg of CB1R or CB2R and 9 μg of pcDNA 3.1+ or AHA1, whereas Neuro-2A cells were transfected with 9 μg pcDNA3.1+ or 9 μg AHA-1. The cells were plated in 24-well plates were serum starved for 24 h. Two days after transfection, the medium was replaced with PBS containing IBMX (100 μM) for 1 h. 10^{-6} M 9-THC was added for 5 min, followed by stimulation with forskolin (10 μM) for 15 min. The reactions

were terminated by addition 1 ml of acetic acid (4%) and the cAMP levels were determined by ELISA.

Determination of CB1R and CB2R levels at the cell surface

CB1R and CB2R levels at the cell surface were determined by ELISA, as described (Rozenfeld et al., 2008, Gomes et al., 2009). In brief, the transfected HEK293T and Neuro-2A cells in 12-well plates were serum starved for 24 h and subsequently fixed with 200 μl methanol for 20 min at −20°C. After three washes with PBS, the cells were incubated with CB1R or CB2R antibodies (Cayman, 1:1,000) for 10 h at 4°C. Subsequently, the cells were washed three times and exposed to secondary antibody (1:1,000) for 2 h at 37°C. After incubation for 15 min with the substrate (OPD[o-Phenylenediamine]) the fluorescence was read at 490 nm. For each experiment, the non-specific fluorescence obtained by omitting the incubation with the secondary antibody was subtracted from the final results.

Fluorescence microscopy

To analyze the subcellular localization of cannabinoid receptors, HEK293T cells were grown on coverslips pre-coated with poly-L-lysine and transfected with 125 ng of 3xHA-tagged receptors, 500 ng DsRed-Rab5, and 500 ng pcDNA3.1+ or AHA1. The cells were fixed with 4% paraformaldehyde–4% sucrose mixture in PBS for 15 min, permeabilized with PBS containing 0.2% Triton X-100 for 5 min, blocked with 5% normal donkey serum for 1 h, followed by incubation with antibodies against HA (Santa Cruz, 1:100) for 2 h. After three washes with PBS, the cells were incubated with Alexa Fluor 594-labeled secondary antibody (1:1000) for 1 h at room temperature and the nucleus was stained with 4, 6-diamidino-2-phenylindole for 5 min. The coverslips were mounted, and fluorescence was detected with a Leica DMRA2 epifluorescent microscope as described (Filipeanu et al., 2006; Filipeanu et al., 2011). Images were deconvolved using SlideBook software and the nearest neighbor deconvolution algorithm (Intelligent Imaging Innovations).

Statistics

Each experiment was repeated at least in three independent transfections and the data are shown as mean ± SD. The statistical differences were tested using using one- or two-way ANOVA followed by Holm Sidak-test or by Student t-test with $p < 0.05$ being considered significantly different.

Results

To determine the long-term effect of adolescent Δ9-THC use on cellular functioning, we performed a proteomic analysis of cerebellar extracts to examine proteins that were modified by both chronic treatment and hormonal status. In these extracts, which comprised 4 groups (intact/saline, intact/THC, OVX/saline, and OVX/THC), we found only six proteins that displayed variations larger than 1.5 fold (Table 1). Two of these proteins, pyruvate carboxylase and NADH dehydrogenase, have mitochondrial localization and were shown to play major roles in cellular energy metabolism; both were decreased by long-term THC administration. The other four proteins are localized predominantly in the cytosol and have different cellular roles. NM23 (NDKB) regulates cell adhesion and migration, transitionally-

controlled-tumor protein modulates cellular proliferation, DJ-1 (PARK-7) is involved in cytoprotection, while AHA1 is a co-chaperone for HSP90.

AHA1 interacts directly with the middle domain of HSP90, according to its ATP binding site, and it is the only HSP90 co-chaperone known to stimulate the ATP-ase activity of heat shock protein (Lotz et al., 2003). Except for cancer cells, there are no data on cellular variations of AHA1 levels in either physiological or pathological conditions. Present results are the first data indicating that drug abuse and estrogen levels may directly regulate this co-chaperone. The proteomic results were further confirmed by western-blot analysis (Fig 1A), which showed that AHA1 levels were significantly increased by $51 \pm 13\%$ by ∆9-THC treatment during adolescence. These levels reached 277 ± 38 % in the group that received both ∆9-THC and ovariectomy (Fig 1A and B). Interestingly, although the levels of AHA1 were increased, we found no changes in the levels of HSP90α or HSP90β in the cerebellum after ∆9-THC or ovariectomy (Fig 1A).

To test if changes in the endogenous levels of AHA1 might change the expression and signaling of cannabinoid receptors, we used a heterologous transfection system in HEK293T cells. Transfection of AHA1 in these cells increased the levels of this protein by 381 ± 45 % over the endogenous levels (n=4, Fig 2A). In addition, AHA1 overexpression significantly enhanced the cell surface levels of CB1R, but it was without effect on CB2R plasma membrane levels (Fig 2B). These results were confirmed by examining the subcellular localization of these receptors using confocal microscopy. In agreement with previous results in transfected HEK293T cells, CB1R was localized both at the plasma membrane and in intracellular organelles, overlapping with the early endosomal marker Rab5 (Fig 2C). In the cells co-transfected with AHA1, however, this pattern was clearly shifted to a plasma membrane localization (Fig 2C). In contrast, the subcellular localization of CB2R was not changed after overexpressing AHA1 (data not shown). Further, in co-immunoprecipitation experiments, interactions between transfected CB1R and endogenous AHA1 were detected (Fig 2D). As expected, these interactions were greatly increased in the HEK293T cells co-transfected with AHA1 (Fig 2D).

The changes in CB1R plasma membrane levels in AHA1 overexpressing cells also affected the amplitude of ∆9-THC-induced cellular signaling. In control cells, pretreatment for 5 min with 10^{-6} M ∆9-THC decreased the cAMP production in response to forskolin by 34 ± 8 %. However, in AHA1 overexpressing cells, the effects of ∆9-THC were significantly larger, as the inhibition of the cAMP levels reach 88 ± 9 % (Fig 3). Like in the case of the cell surface expression, AHA1 overexpression did not change the effects of ∆9-THC on CB2R modulation of cAMP levels (Fig 3). The overexpression of AHA1 not only changed the effects of ∆9-THC on cAMP levels, but also on MAPK phosphorylation (Fig 4). Again, no differences were observed for the effects of ∆9-THC on the CB2R mediated MAPK phosphorylation between control and AHA1 overexpressing cells (data not shown).

CB1R is endogenously expressed in the Neuro-2A neuroblastoma cell line (Rozenfeld and Devi, 2008). Overexpression of AHA1 in this cell line (Fig 5A) increased the CB1R cell surface levels by 67 ± 11 % (Fig 5B). Further, the effects of ∆9-THC on the forskolin-

stimulated cAMP levels were significantly enhanced in Neuro-2A cells overexpressing AHA1 (Fig 5C).

Discussion

The endocannabinoid system consists of endogenous ligands and the enzymes involved in their metabolism and these ligands exert multiple patho-physiological roles by activation of CB1R and CB2R. However, these receptors can also be activated by 9-THC, the main psychoactive component of marijuana and hashish (Mechoulam 1986, Mackie 2008; Cabral et al., 2008; Bosier et al 2010, Turu and Hunyady, 2010). The widespread use of this drug for recreational purposes, as well as the recently proposed therapeutic potential in AIDS and terminal cancers, raises important and controversial political and economic issues (Seamon et al., 2007; Molina et al, 2011).

Although our knowledge on the regulation of CB1R and CB2R expression, trafficking, and signaling at the cellular level has greatly advanced during the last decade, the effects of chronic 9-THC *in vivo* are still largely unknown. The present study is among the first to directly address this question. Our results indicate that chronic 9-THC specifically upregulates a limited number proteins in cerebellum. Recently, another study was published on the transcriptomic and proteomic changes induced by 9-THC in the mouse cerebellum (Colombo et al., 2009). However, in that study, drug administration was limited to only 4.5 days. This short-term treatment is the most likely explanation for the differences between the data obtained in these two studies. In our protocol, chronic 9-THC lasted for 40 days during adolescence and it was followed by acute challenges with 9-THC for 70 days during adulthood to assess any long-term changes in its behavioral and pharmacodynamic effects (Winsauer et al., 2011). In addition, our study was conducted with both intact and ovariectomized females to examine the interaction of ovarian hormones and chronic 9-THC administration. The results from this study were limited to the proteins that varied in all four of our treatment groups (Table 1). Nevertheless, our data together with the previous study (Colombo et al., 2009) suggest that the effects of 9-THC effects on protein expression may depend on the duration of use and show that the expression of certain proteins involved in a variety of cellular functions, such as energy metabolism, cell adhesion, cytoprotection and intracellular protein transport were changed.

Pyruvate carboxylase mediates the carboxylation of pyruvate to form oxaloacetate (Jitrapakdee S, et al., 2008) and is expressed in the CNS, including the cerebellum (Ghandour et al., 2000), where its activity can be changed by convulsive drugs (Eloqayli et al., 2004). NADH dehydrogenase, which was also found to decrease during 4.5 days of 9-THC administration (Colombo et al, 2009), is a member of complex I mitochondrial transport and supports ATP formation and transport of metabolites (Hirst, 2010) and the impairment of mitochondrial complex I was proposed to play a role in the etiology of Parkinson's disease (Marella et al., 2009). This observation may be relevant considering that in the present study chronic 9-THC increased another protein, DJ-1 (PARK7), which is mutated in about 1% of recessive Parkinson cases (da Costa 2007). Right now, no population studies are available to correlate the use of marijuana with the incidence of Parkinson disease. Still, our proteomic data indicate that chronic 9-THC may regulate the levels of

specific proteins involved in the etiology of Parkinson's disease and these observations require further investigation.

NM23B belongs to a family of nucleoside diphosphate kinases and members of this family are involved in proliferation, differentiation, molecular transport, and apoptosis (Bosnar et al., 2009). The interest in this group of proteins is due to their potential role in the suppression of metastasis (Bosnar et al., 2009; Marshall et al., 2010), but at present, there are no reports on the regulation of their endogenous levels by GPCR activation, particularly by CB1R or CB2R. Our data indicate that the expression of NM23B is enhanced in cerebellum by chronic Δ9-THC. In addition, another oncogene has been found to be changed by chronic Δ9-THC, translationally controlled-tumor protein. Overexpression of TCTP in mammalian cells resulted in slow growth and a delay in cell cycle progression (Gachet et al., 1999), whereas down-regulation of TCTP expression was found to be associated with reversion of cells from the transformed to the normal phenotype. However, TCTP is not a tumor specific protein, although its endogenous levels tend to be higher in cancer cells. In CNS, changes in TCTP levels have been detected in certain areas of postmortem brains from Down syndrome and Alzheimer's patients (Kim et al., 2001).

AHA1 is a HSP90 co-chaperone that increases its ATP-ase activity (Lotz et al., 2003; Wang et al., 2006). The proteomic analysis demonstrated that chronic Δ9-THC increased AHA1 levels in the cerebellum. We selected AHA1 to characterize its role in the regulation of cannabinoid receptor expression and signaling further, because this co-chaperone has been demonstrated to regulate intracellular protein traffic, at least in the case of ΔF508 CFTR mutant (Wang et al., 2006). In addition, we recently demonstrated that HSP90 is essential in the temperature-dependent α_{2C}-AR intracellular trafficking (Filipeanu et al., 2011) and the interaction between CB2R and HSP90 are required for receptor mediated $G_{\alpha}i$-Rac interactions (He et al., 2007).

Heat shock proteins (HSP) were identified in 1962 as a set of highly conserved molecules, representing one of the largest families of molecular chaperones (Ritossa 1962). HSP are expressed constitutively in the cells, but these levels are largely enhanced by cellular stressors. Subsequently, HSP are involved in many cytoprotective roles by controlling the nascent protein folding and inhibiting the formation of protein aggregates. Based on the molecular weight, there are six distinct classes of HSP, each of them with specific cellular functions. The HSP90 subfamily is formed from at least four distinct members, HSP90α and β are localized in the cytosol, GRP94 is present in the endoplasmic reticulum and TRAP1 is a mitochondrial protein (Taherian et al., 2008). Unlike the HSP70 subfamily, the cytosolic HSP90α and β isoforms have a distinct repertoire of specific 'client' proteins with which they interact, playing the role of scaffold and regulating the maturation and signaling of these molecules (Pearl et al., 2008; Taherian et al., 2008; Filipeanu et al., 2011). The cytosolic HSP90 isoforms operate as part of multimeric chaperone complex and their activity is dependent on the presence of specific co-chaperones like HOP, p23, p50, CDC37, UNC45 and AHA1. Among these co-chaperones, AHA1 increases the ATP-ase activity of HSP90 by about 10 fold by binding to the middle domain of the α and β HSP90 isoforms (Pearl et al., 2008; Taherian et al., 2008). However, AHA1 cannot prevent the aggregation of misfolded proteins, and thus, does not act directly as a chaperone (Lotz et al., 2003). Still,

downregulation of endogenous AHA1 levels promotes the trafficking of the misfolded F508 CFTR mutant to the cell surface and increases the sensitivity of cancer cells to HSP90 inhibitors (Wang et al., 2006; Holmes et al., 2010). Currently, very little is known about the regulation of endogenous AHA1, although differences have been observed in certain cancer cell lines, but endogenous levels of AHA1 do not correlate with the expression levels of HSP90 and HSP70 (Holmes et al., 2010). However, in the HT29 colonic carcinoma cell line, increased AHA1 levels are accompanied by an enhancement in protein phosphorylation that does not affect the sensitivity to HSP90 inhibitors (Holmes et al., 2010).

Our data are the first demonstration of the modulation of endogenous AHA1 levels outside of cancer cell biology. The proteomic findings were confirmed by western-blotting, which showed that chronic 9-THC during adolescence increased the co-chaperone levels in the cerebellum of adult animals. Interestingly, ovariectomy also increased AHA1 levels, indicating that the levels of specific molecular chaperones are also controlled by the gonadal hormones. However, we did not find changes in the expression of HSP90 α and β (Fig 2), indicating that in the case of chronic 9-THC and ovariectomy, the putative changes in the activity of these HSP occurr by modulating the expression of the co-chaperones. Whether or not the observed effects occurred in other regions of the brain, or are limited to the cerebellum, remains to be determined.

Given that endogenous levels of AHA1 have been shown to modulate the levels of 508F CFTR mutant at the plasma membrane (Wang et al., 2006), we wanted to determine whether AHA1 overexpression changed the subcellular localization and signaling of CB1R and CB2R. Most cannabinoid ligands are highly lipophilic, and diffuse through biological membranes and may stimulate intracellularly localized cannabinoid receptors (Oz, 2006; Reggio, 2010). Recent data have also suggested that the signaling and cellular effects resulting from the stimulation of these intracellular receptors may be different from the stimulation of plasma membrane receptors (Rozenfeld and Devi, 2008; Rozenfeld, 2011). At least in the case of CB1R, there is clear evidence that are present in the early endosomes due to interactions with AP-3 (Rozenfeld and Devi 2008). In the present study, we found that AHA1 overexpression shifted the subcellular receptor localization toward the plasma membrane, and increased the effects of 9-THC on cAMP levels and MAPK activation. More important, these effects were specific for CB1R as AHA1 overexpression had no effects on the plasma membrane levels or signaling of CB2R. The effects of AHA1 on CB1R subcellular localization and signaling are not limited to transfected HEK293T cells, as increases in AHA1 levels had a similar effect in Neuro-2A cells. Overall, the data obtained in these cell lines indicate that increasing cellular levels of AHA1 enhances plasma membrane levels of CB1R and the acute effects of 9-THC on cellular function. These data differ from our previous results (Winsauer et al., 2011) demonstrating that chronic 9-THC reduced CB1R levels in the hippocampus and striatum. One explanation for this difference may be that our previous study only measured the total levels of CB1R in a mixed cell population composed of neurons, glial and microglial cells. Thus, chronic 9-THC may have differential effects on the regulation of cannabinoid receptor expression depending on the cell type and specific molecular chaperones expressed by each cell type. Alternatively, chronic 9-THC may change the subcellular distribution of cannabinoid receptors by

decreasing the total cellular levels, but enhancing the plasma membrane receptor localization. Lastly, alterations in the cellular levels of AHA1 may be just one of the many mechanisms involved in intracellular CB1R trafficking and the effects of other molecular chaperones may predominate or account for the final variations in the CB1R levels observed *in vivo*. Whether or not the actions of AHA-1 on CB1R trafficking and signaling are the direct consequence of changes in the HSP90 chaperoning activity remains the aim of further studies. However, this hypothesis is supported by the recent results showing that HSP90 phosphorylation at a specific threonine residue decreased its interactions with other co-chaperones, but AHA-1 overexpression prevented this effect.

In conclusion, the present investigation demonstrated that chronic administration of 9-THC induced changes in the endogenous levels of a specific subset of proteins in the cerebellum of female rats. These changes were also modulated by ovariectomy, supporting our previous finding that the long-term effects of cannabinoids can depend on hormonal status. The effects of chronic 9-THC on specific molecular chaperones may modify the expression and signaling of the cannabinoid receptors, as observed in the present study for AHA1.

Acknowledgments

References

Alban A, David SO, Bjorkesten L, Andersson C, Sloge E, Lewis S, Currie I. A novel experimental design for comparative two-dimensional gel analysis: two-dimensional difference gel electrophoresis incorporating a pooled internal standard. Proteomics. 2003; 3:36–44. [PubMed: 12548632]

Bosier B, Muccioli GG, Hermans E, Lambert DM, et al. Functionally selective cannabinoid receptor signalling: therapeutic implications and opportunities. Biochem Pharmacol. 2010; 80:1–12. [PubMed: 20206137]

Bosnar MH, Bago R, Cetkovi H, et al. Subcellular localization of Nm23/NDPK A and B isoforms: a reflection of their biological function? Mol Cell Biochem. 2009; 329:63–71. [PubMed: 19373546]

Cabral GA, Raborn ES, Griffin L, Dennis J, Marciano-Cabral F, et al. CB2 receptors in the brain: role in central immune function. Br J Pharmacol. 2008; 153:240–251. [PubMed: 18037916]

Colombo G, Rusconi F, Rubino T, Cattaneo A, Martegani E, Parolaro D, Bachi A, Zippel R, et al. Transcriptomic and proteomic analyses of mouse cerebellum reveals alterations in RasGRF1 expression following in vivo chronic treatment with delta 9-tetrahydrocannabinol. J Mol Neurosci. 2009; 37:111–122. [PubMed: 18584336]

Childers SR, et al. Activation of G-proteins in brain by endogenous and exogenous cannabinoids. AAPS J. 2006; 8:E112–E117. [PubMed: 16584117]

Cooray SN, Chan L, Webb TR, Metherell L, Clark AJ, et al. Accessory proteins are vital for the functional expression of certain G protein-coupled receptors. Mol Cell Endocrinol. 2009; 300:17–24. [PubMed: 19000738]

Cudaback E, Marrs W, Moeller T, Stella N, et al. The expression level of CB1 and CB2 receptors determines their efficacy at inducing apoptosis in astrocytomas. PLoS One. 2010; 5:e8702. [PubMed: 20090845]

da Costa CA, et al. DJ-1: a newcomer in Parkinson's disease pathology. Curr Mol Med. 2007; 7:650–657. [PubMed: 18045143]

Daniel JM, Winsauer PJ, Brauner IN, Moerschbaecher JM, et al. Estrogen improves response accuracy and attenuates the disruptive effects of delta9-THC in ovariectomized rats responding under a

multiple schedule of repeated acquisition and performance. Behav Neurosci. 2002; 116:989–998. [PubMed: 12492298]

DeWire SM, Ahn S, Lefkowitz RJ, Shenoy SK, et al. Beta-arrestins and cell signaling. Annu Rev Physiol. 2007; 69:483–510. [PubMed: 17305471]

Dong C, Filipeanu CM, Duvernay MT, Wu G, et al. Regulation of G protein-coupled receptor export trafficking. Biochim Biophys Acta. 2007; 1768:853–870. [PubMed: 17074298]

Dunham JH, Hall RA, et al. Enhancement of the surface expression of G protein-coupled receptors. Trends Biotechnol. 2009; 27:541–545. [PubMed: 19679364]

Duvernay MT, Filipeanu CM, Wu G, et al. The regulatory mechanisms of export trafficking of G protein-coupled receptors. Cell Signal. 2005; 17:1457–1465. [PubMed: 16014327]

Eloqayli H, Dahl CB, Götestam KG, Unsgård G, Sonnewald U, et al. Changes of glial-neuronal interaction and metabolism after a subconvulsive dose of pentylenetetrazole. Neurochem Int. 2004; 45:739–745. [PubMed: 15234117]

Filipeanu CM, de Zeeuw D, Nelemans SA, et al. Delta9-tetrahydrocannabinol activates [Ca2+]i increases partly sensitive to capacitative store refilling. Eur J Pharmacol. 1997; 336:R1–R3. [PubMed: 9384260]

Filipeanu CM, Zhou F, Claycomb WC, Wu G, et al. Regulation of the cell surface expression and function of angiotensin II type 1 receptor by Rab1-mediated endoplasmic reticulum-to-Golgi transport in cardiac myocytes. J Biol Chem. 2004; 279:41077–41084. [PubMed: 15252015]

Filipeanu CM, Zhou F, Lam ML, Kerut KE, Claycomb WC, Wu G, et al. Enhancement of the recycling and activation of beta-adrenergic receptor by Rab4 GTPase in cardiac myocytes. J Biol Chem. 2006; 281:11097–11103. [PubMed: 16484224]

Filipeanu CM, de Vries R, Danser AH, Kapusta DR, et al. Modulation of α(2C) adrenergic receptor temperature-sensitive trafficking by HSP90. Biochim Biophys Acta. 2011; 1813:346–357. [PubMed: 21145921]

Gachet Y, Tournier S, Lee M, Lazaris-Karatzas A, Poulton T, Bommer UA, et al. The growth-related, translationally controlled protein P23 has properties of a tubulin binding protein and associates transiently with microtubules during the cell cycle. J Cell Sci. 1999; 112:1257–1271. [PubMed: 10085260]

Ghandour MS, Parkkila AK, Parkkila S, Waheed A, Sly WS, et al. Mitochondrial carbonic anhydrase in the nervous system: expression in neuronal and glial cells. J Neurochem. 2000; 75:2212–2220. [PubMed: 11032910]

Gomes I, Grushko JS, Golebiewska U, Hoogendoorn S, Gupta A, Heimann AS, Ferro ES, Scarlata S, Fricker LD, Devi LA, et al. Novel endogenous peptide agonists of cannabinoid receptors. FASEB J. 2009; 23:3020–3029. [PubMed: 19380512]

Godlewski G, Offertáler L, Wagner JA, Kunos G, et al. Receptors for acylethanolamides-GPR55 and GPR119. Prostaglandins Other Lipid Mediat. 2009; 89:105–111. [PubMed: 19615459]

He F, Qiao ZH, Cai J, Pierce W, He DC, Song ZH, et al. Involvement of the 90-kDa heat shock protein (Hsp-90) in CB2 cannabinoid receptor-mediated cell migration: a new role of Hsp-90 in migration signaling of a G protein-coupled receptor. Mol Pharmacol. 2007; 72:1289–1300. [PubMed: 17698952]

Herkenham M, Lynn AB, Little MD, Johnson MR, Melvin LS, de Costa BR, Rice KC, et al. Cannabinoid receptor localization in brain. Proc Natl Acad Sci U S A. 1990; 87:1932–1936. [PubMed: 2308954]

Herkenham M, Lynn AB, Johnson MR, Melvin LS, de Costa BR, Rice KC, et al. Characterization and localization of cannabinoid receptors in rat brain: a quantitative in vitro autoradiographic study. J Neurosci. 1991; 11:563–583. [PubMed: 1992016]

Heimann AS, Gomes I, Dale CS, Pagano RL, Gupta A, de Souza LL, Luchessi AD, Castro LM, Giorgi R, Rioli V, Ferro ES, Devi LA, et al. Hemopressin is an inverse agonist of CB1 cannabinoid receptors. Proc Natl Acad Sci U S A. 2007; 104:20588–20593. [PubMed: 18077343]

Hirst J, et al. Towards the molecular mechanism of respiratory complex I. Biochem J. 2009; 425:327–339. [PubMed: 20025615]

Holmes JL, Sharp SY, Hobbs S, Workman P, et al. Silencing of HSP90 cochaperone AHA1 expression decreases client protein activation and increases cellular sensitivity to the HSP90 inhibitor 17-allylamino-17-demethoxygeldanamycin. Cancer Res. 2008; 68:1188–1197. [PubMed: 18281495]

Jitrapakdee S, St Maurice M, Rayment I, Cleland WW, Wallace JC, Attwood PV, et al. Structure, mechanism and regulation of pyruvate carboxylase. Biochem J. 2008; 413:369–387. [PubMed: 18613815]

Kim SH, Cairns N, Fountoulakisc M, Lubec G, et al. Decreased brain histamine-releasing factor protein in patients with Down syndrome and Alzheimer's disease. Neurosci Lett. 2001; 300:41–44. [PubMed: 11172935]

Leterrier C, Bonnard D, Carrel D, Rossier J, Lenkei Z, et al. Constitutive endocytic cycle of the CB1 cannabinoid receptor. J Biol Chem. 2004; 279:36013–36021. [PubMed: 15210689]

Lotz GP, Lin H, Harst A, Obermann WM, et al. Aha1 binds to the middle domain of Hsp90, contributes to client protein activation, and stimulates the ATPase activity of the molecular chaperone. J Biol Chem. 2003; 278:17228–17335. [PubMed: 12604615]

Luo S, Zhang B, Dong XP, Tao Y, Ting A, Zhou Z, Meixiong J, Luo J, Chiu FC, Xiong WC, Mei L, et al. HSP90 beta regulates rapsyn turnover and subsequent AChR cluster formation and maintenance. Neuron. 2008; 60:97–110. [PubMed: 18940591]

Mackie K, et al. Cannabinoid receptors: where they are and what they do. J Neuroendocrinol. 2008; 20:10–14. [PubMed: 18426493]

Marella M, Seo BB, Yagi T, Matsuno-Yagi A, et al. Parkinson's disease and mitochondrial complex I: a perspective on the Ndi1 therapy. J Bioenerg Biomembr. 2009; 41:493–497. [PubMed: 19904590]

Marshall JC, Collins J, Marino N, Steeg P, et al. The Nm23-H1 metastasis suppressor as a translational target. Eur J Cancer. 2010; 46:1278–1282. [PubMed: 20304626]

Mechoulam, R. The pharmacology of cannabis sativa. In: Mechoulam, R., editor. Cannabinoids as Therapeutic Agents. Boca Raton, FL: CR; 1986. p. 1-19.

Molina PE, Winsauer P, Zhang P, Walker E, Birke L, Amedee A, Stouwe CV, Troxclair D, McGoey R, Varner K, Byerley L, Lamotte L, et al. Cannabinoid Administration Attenuates the Progression of Simian Immunodeficiency Virus. AIDS Res Hum Retroviruses. 2011; 27:585–592. [PubMed: 20874519]

Mollapour M, Tsutsumi S, Truman AW, Xu W, Vaughan CK, Beebe K, Konstantinova A, Vourganti S, Panaretou B, Piper PW, Trepel JB, Prodromou C, Pearl LH, Neckers L, et al. Threonine 22 phosphorylation attenuates Hsp90 interaction with cochaperones and affects its chaperone activity. Mol Cell. 2011; 41:672–681. [PubMed: 21419342]

Matsumoto A, et al. Synaptogenic action of sex steroids in developing and adult neuroendocrine brain. Psychoneuroendocrinology. 1991; 16:25–40. [PubMed: 1961842]

Oz M, et al. Receptor-independent actions of cannabinoids on cell membranes: focus on endocannabinoids. Pharmacol Ther. 2006; 111:114–144. [PubMed: 16584786]

Pearl LH, Prodromou C, Workman P, et al. The Hsp90 molecular chaperone: an open and shut case for treatment. Biochem J. 2008; 410:439–453. [PubMed: 18290764]

Pope HG Jr, Jacobs A, Mialet JP, Yurgelun-Todd D, Gruber S, et al. Evidence for a sex-specific residual effect of cannabis on visuospatial memory. Psychother Psychosom. 1997; 66:179–184. [PubMed: 9259040]

Ramos RR, Swanson AJ, Bass J, et al. Calreticulin and Hsp90 stabilize the human insulin receptor and promote its mobility in the endoplasmic reticulum. Proc Natl Acad Sci U S A. 2007; 104:10470–10475. [PubMed: 17563366]

Reggio PH, et al. Endocannabinoid binding to the cannabinoid receptors: what is known and what remains unknown. Curr Med Chem. 2010; 17:1468–1486. [PubMed: 20166921]

Ritossa F, et al. A new puffing pattern induced by temperature shock and DNP in. Drosophila Experientia. 1962; 18:571–573.

Rozenfeld R, Devi LA, et al. Regulation of CB1 cannabinoid receptor trafficking by the adaptor protein AP-3. FASEB J. 2008; 22:2311–2322. [PubMed: 18267983]

Rozenfeld R, et al. Type I cannabinoid receptor trafficking: all roads lead to lysosome. Traffic. 2011; 12:12–18. [PubMed: 21040297]

Seamon MJ, Fass JA, Maniscalco-Feichtl M, Abu-Shraie NA, et al. Medical marijuana and the developing role of the pharmacist. Am J Health Syst Pharm. 2007; 64:1037–1044. [PubMed: 17494903]

Taherian A, Krone PH, Ovsenek N, et al. A comparison of Hsp90alpha and Hsp90beta interactions with cochaperones and substrates. Biochem Cell Biol. 2008; 86:37–45. [PubMed: 18364744]

Thompson DM, Moerschbaecher JM, et al. Operant methodology in the study of learning. Environ Health Perspect. 1978; 26:77–87. [PubMed: 102510]

Turu G, Hunyady L, et al. Signal transduction of the CB1 cannabinoid receptor. J Mol Endocrinol. 2010; 44:75–85. [PubMed: 19620237]

Tuusa JT, Markkanen PM, Apaja PM, Hakalahti AE, Petäjä-Repo UE, et al. The endoplasmic reticulum Ca2+-pump SERCA2b interacts with G protein-coupled receptors and enhances their expression at the cell surface. J Mol Biol. 2007; 371:622–638. [PubMed: 17588601]

Wang X, Venable J, LaPointe P, Hutt DM, Koulov AV, Coppinger J, Gurkan C, Kellner W, Matteson J, Plutner H, Riordan JR, Kelly JW, Yates JR, Balch WE, et al. Hsp90 cochaperone Aha1 downregulation rescues misfolding of CFTR in cystic fibrosis. Cell. 2006; 127:803–815. [PubMed: 17110338]

Winsauer PJ, Daniel JM, Filipeanu CM, Leonard ST, Hulst JL, Rodgers SP, Lassen-Greene CL, Sutton JL. Long-term behavioral and pharmacodynamic effects of delta-9-tetrahydrocannabinol in female rats depend on ovarian hormone status. Addict Biol. 2011; 16:64–81. [PubMed: 21158010]
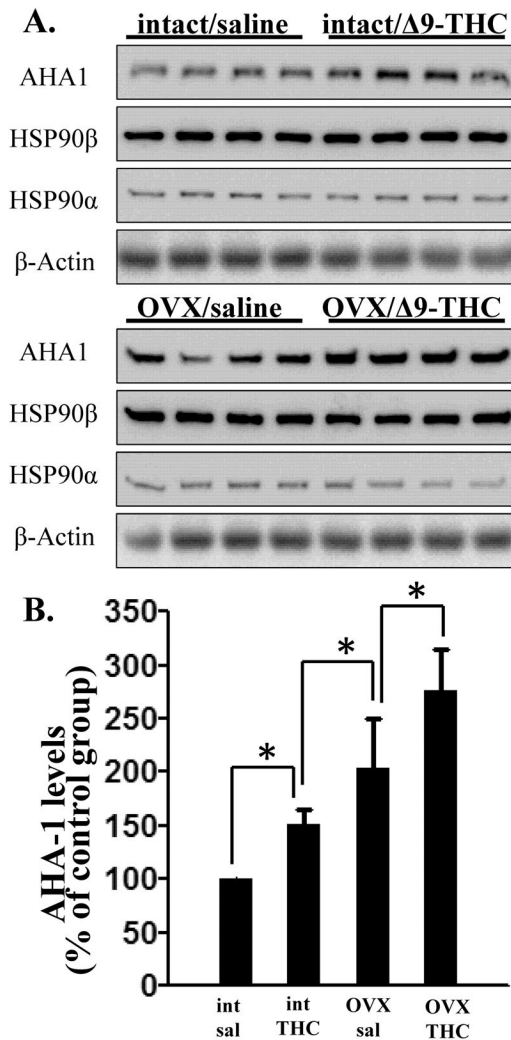
A.

Figure 1. The effects of chronic Δ9-THC on the endogenous levels of AHA1 in rat cerebellum
A. Western blots of AHA1 levels in the cerebellar extracts from intact or ovariectimized female rats administered either saline or Δ9-THC during adolescence. The cerebellar extracts (20 μg/lane) were separated by 10% SDS-PAGE, transferred onto PDVF membranes, and subjected to western-blotting with specific antibodies. The data were quantified using a Fuji Film luminescent image analyzer (LAS-1000 Plus) and the Image Gauge program (Version 3.4). B. Quantification for the experiments shown in A. AHA1 levels were corrected for the β-actin levels in the same samples and the data are presented as the % from the levels found in the control group. *- indicate statistical significant differences between the four groups with $p < 0.05$.
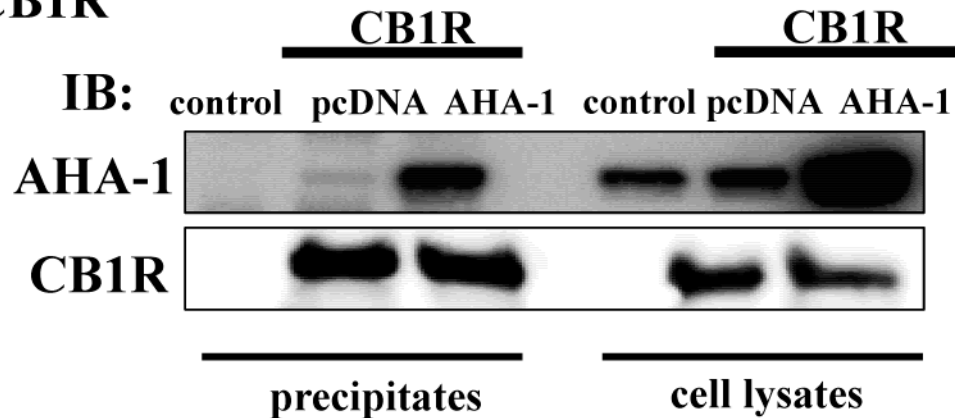
A.

B.

C.
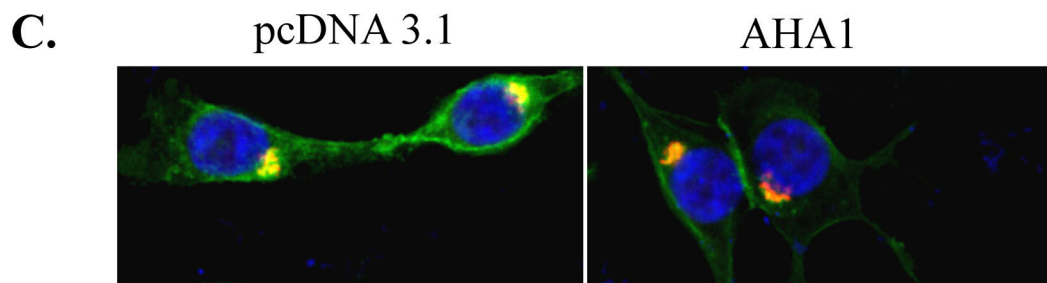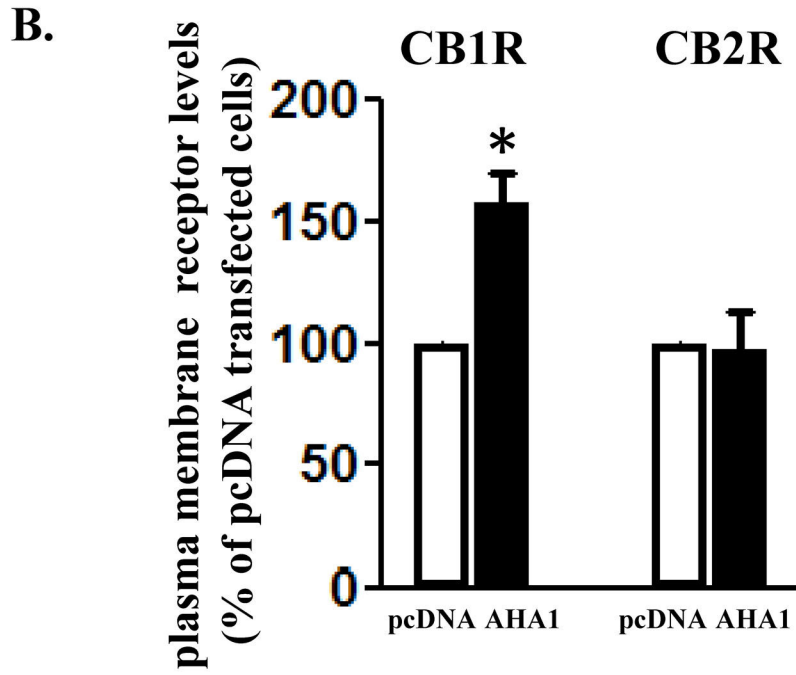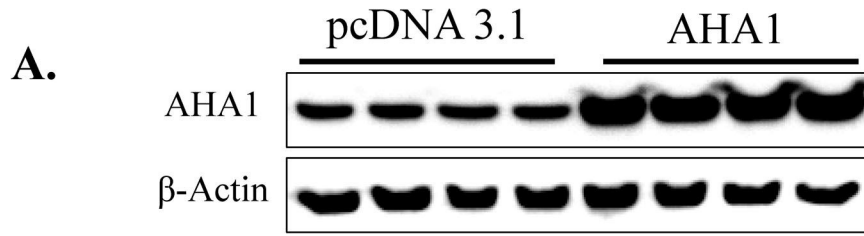
Figure 2. The effects of AHA1 overexpression on the subcellular localization of CB1R and CB2R in HEK293T cells

A. AHA-1 levels in control and AHA-1 transfected HEK293T cells. The cells were transfected with pcDNA 3.1 or AHA-1 (2.25 μg/well in 6-well plates) and serum starved for 24 h. Two days after transfection the cells were lysated and 10 μg of total protein were separated by 10% SDS-PAGE and AHA-1 levels were determined by western blot. B. Modulation of CB1R and CB2R plasma membrane levels by AHA1 overexpression. HEK293T were co-transfected with CB1R or CB2R (0.25 μg/well) and pcDNA 3.1 or AHA-1 (2.25 μg/well each) and after six hours the cells were trypsinized and plated on 12-well plates as described in Material and Methods. FBS was withdrawn for 24 h, and two days after transfection the plasma membrane levels of CB1R and CB2R were determined by ELISA as described in Material and Methods. n=12 in each case from three different transfections. *- indicate $p < 0.05$ compared to pcDNA 3.1 transfected cells. C. Subcellular localization of CB1R in HEK293T cells. The cells were grown on coverslips in 6-well plates and transfected with 3xHA-CB1R (0.1 μg/well) and DsRed-Rab5 (0.1 μg/well). After serum starvation for 24 h, the cells were fixed and permeabilized. The CB1R localization was stained using HA antibody as described in Material and Methods. Blue: DNA staining by 4,6-diamidino-2-phenylindole (nuclear), green: 3xHA-CB1R, red: DsRed-Rab5. The images are representative from three different coverslips, obtained from three independent transfections. D. CB1R interacts with AHA-1 in HEK293T cells. The cells were transiently co-transfected in 10 mm^2 dishes with pcDNA 3.1 (10 μg, control), or with CB1R (5 μg) and pcDNA3.1 (5 μg), or CB1R (5 μg) and AHA-1 (5 μg). After two days the cells were solubilized and immunoprecipitated with CB1R antibody as described under Material and Methods. The immunoprecipitates (20 μg/lane) or the lysates (10 μg/lane) were separated by 10 % SDS-Page and subject to western-blotting with AHA-1 and CB1R antibodies. The experiment shown is representative from three independent transfections.
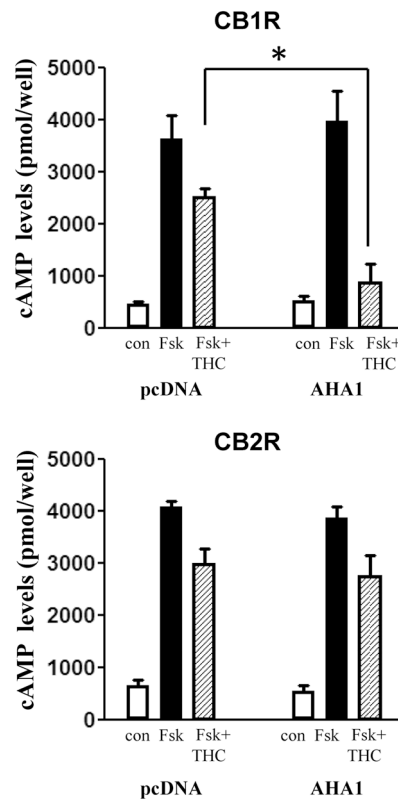
Figure 3. The effects of AHA1 overexpression on the CB1R and CB2R modulation of cAMP levels in HEK293T cells

HEK293T co-transfected with CB1R or CB2R and pcDNA3.1 or AHA1 as in Fig 2B were plated on 24 well-plates and serum straved for 24h. Two days after transfection the medium was changed to PBS containing 100 μM IBMX for one hour. Subsequently, the cells were pretreated with   9-THC (1 μM)) for 5 min, followed by stimulation with forskolin (10 μM) for 15 min. The reactions were stopped by medium aspiration and addition of 200 μl thhricloracetic acid. cAMP levels were determined using cAMP Elisa Kit (Cayman Biochemicals) as described in Material and Methods. n=12 in each case from three independent transfections. *- indicates statistically significant differences between pcDNA 3.1 and AHA1 transfected cells by two-way ANOVA followed by Holm Sidak-test (interaction: $F(2,12=14.03, p<0.001)$.
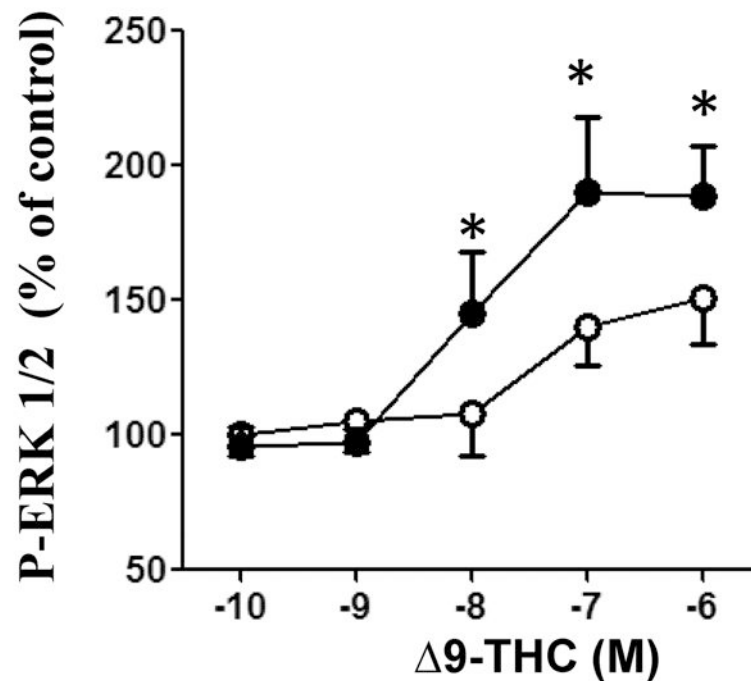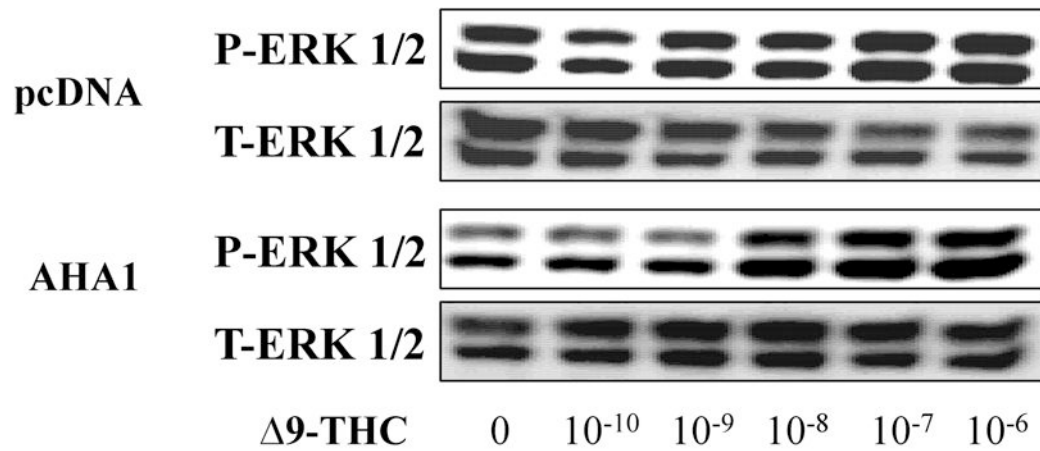
Figure 4. The effects of AHA1 overexpression on CB1R-mediated MAPK activation
HEK293T cells in 6-well plates were co-transfected with CB1R (0.25/μg/well) and pcDNA 3.1 or AHA1 (each at 2.25 μg/well). Subsequently, the cells were serum starved for 24 h and then stimulated with increasing concentrations of 9-THC for 5 min. The reactions were stopped by aspiration of the medium and addition of 200 μl lysis buffer. Ten μg of protein were separated by SDS-page and ERK 1/2 activation and total ERK 1/2 levels were detected using specific antibodies. Top panel: representative blots from four different experiments. Lower panel: Quantification of the effects of 9-THC on MAPK levels, open symbols indicate pcDNA 3.1 transfected cells and black symbols indicate AHA1 overexpressing

cells; n=4 in each case from four different transfections, * indicates statistically significant differences compared to pcDNA 3.1 transfected cells by one-way ANOVA.
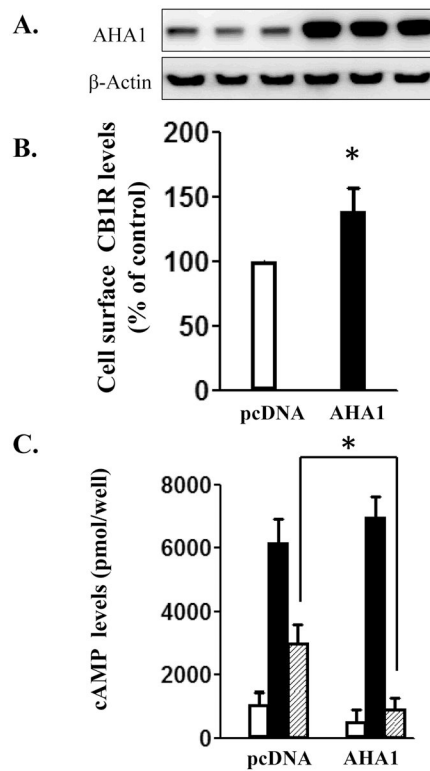
Figure 5. The effects of AHA1 overexpression on the plasma membrane levels and signaling of endogenous CB1R in Neuro-2A cells

A. AHA-1 levels in control and AHA-1 transfected Neuro-2A cells. The cells were transfected with pcDNA 3.1 or AHA-1 (2.25 μg/well in 6-well plates) and serum starved for 24 h. The lysates and the western blot were performed as described in Fig 2A. B. Cell surface levels of CB1R in Neuro-2A overexpressing cells. Neuro2-A cells were transfected as above and then trypsinized and plated at a density of 50×10^4 cells/well in 12-well plates. Subsequent procedures to determine plasma membrane CB1R levels were similar to that described for HEK293T cells in Fig 2B. n=9 from three different experiments. * indicates statistically significant differences compared to pcDNA 3.1 transfected cells. C. The effects of CB1R stimulation on cAMP levels in pcDNA 3.1 or AHA-1 transfected Neuro-2A cells. The transfections were made as described and subsequently, the cAMP determinations were conducted as described in the Fig 3. n=12 in each case from three different transfections; * - indicates statistically significant differences between pcDNA 3.1 and AHA1 transfected cells by two-way ANOVA followed by Holm Sidak-test (interaction: F(2,12=30.98, p<0.001).

Table 1

Proteins differentially regulated by chronic Δ9-THC in intact and ovarectomized rats

DeCyder software (GE Healthcare) was used for simultaneous comparison of abundance changes across all samples' 2-DE gels, and for comparisons of individual Cy3 and Cy5 samples for each rat. The DeCyder differential in-gel analysis (DIA) module was used for pair-wise comparisons of each sample on a gel to the Cy2 labeled standard present on each gel. For each pair-wise DIA comparison, the entire signals from each CyDye channel are normalized prior to the co-detection of protein spot boundaries and the calculation of the volume ratio for each protein spot. The DeCyder biological variation analysis (BVA) module was then used to simultaneously match all protein spot maps from all gels, and using the Cy3/Cy5:Cy2 DIA ratios, calculate abundance changes and paired Student's t-test p-values for the variance of these ratios for each protein pair across all samples. In the absence of sufficient experimental replicates, no statistical information can be generated. Fold abundance changes are reported, whereby a fold increase is calculated directly from the volume ratio, and a fold decrease by the inverse of volume ratio. The DIA module was also used to calculate the direct Cy5:Cy3 volume ratio for each paired sample individually (without the Cy2 mixed standard) to assess the contribution from each subject and reveal changes that were present in a group. After determining spots of interest, the protein were excised using the Ettan Spot Handling Workstation with a 2-mm diameter spot-picking head (GE Healthcare). Gel spots were cut, de-stained and then digested with trypsin (Promega). The resulting peptide mixture was loaded on a Dionex PepMap C18 trap column and was separated by a New Objective reversed phase C18 Picofrit column/emitter. Peptide mass was determined by a Thermo-Fisher LTQXL linear ion trap mass spectrometer (Waltham, MA, USA) coupled with an Eksigent nanoLC (Dublin, CA, USA). The raw data were analyzed by the Mascot search engine V2.2 (Matrix Science Inc, Boston, MA, USA) against the rat SwissProt database (false discovery rate <5%) to generate a list of possible proteins for that gel spot.

| Matched Protein[1] | Accession[1] | Protein Score | Peptides Matched | Coverage (%) | Differences (expressed as a ratio to intact/ saline grup) | | | | |
					Intact/ 9-THC	OVX/saline	OVX/ 9-THC	1-ANOVA	Subcellular Localization[1]
pyruvate carboxylase	P52873 (PYC_RAT)	254	36	43	0.79	0.60	0.46	0.0075	mitochondria
NADH dehydrogenase	Q561S0 (NDUAA_RAT)	595	19	47	0.87	0.56	2.51	0.4100	mitochondria,
NM23 (NDKB)	P19804 (NDKB_RAT)	165	9	57	1.70	2.24	3.31	0.0480	cytosol, plasma membrane
translationally controlled tumor protein (TCTP)	P63029 (TCTP_RAT)	90	6	39	0.62	2.29	2.82	0.0330	cytosol
DJ-1 (PARK-7)	O88767 (PARK7_RAT)	127	16	73	1.78	2.14	2.24	0.0240	cytosol, nucleus
AHA1	B0BN63 (AHSA1_RAT)	298	12	49	1.26	2.09	1.55	0.0430	cytosol, ER

[1] - Matched Protein, Accession and Subcellular Localization information as listed in The Universal Protein Resource (The Uniprot Consortium, 2010)